ARCHIVES
Of
FOUNDRY ENGINEERING

ISSN (1897-3310)
Volume 11
Special Issue
2/2011
117–123

23/2

Published quarterly as the organ of the Foundry Commission of the Polish Academy of Sciences

Numerical modelling of liquid material flow in the fusion zone of hybrid welded joint

M. Kubiak *
Department of Mechanics and Machine Design Foundations,
Czestochowa University of Technology, Dabrowskiego 73, 42-200 Czestochowa, Poland
*Corresponding author. E-mail address: kubiak@imipkm.pcz.pl

Received 11.04.2011; Approved for print on: 26.04.2011

Abstract

This paper concerns modelling of liquid metal motion in the fusion zone of laser-arc hybrid butt-welded plate. Velocity field in the fusion zone and temperature field in welded plate were obtained on the basis of the solution of mass, momentum and energy conservations equations. Differential equations were solved using Chorin's projection method and finite volume method. Melting and solidification processes were taken into account in calculations assuming fuzzy solidification front where fluid flow is treated as a flow through porous medium. Double-ellipsoidal heat source model was used to describe electric arc and laser beam heat sources. On the basis of developed solution algorithms simulation of hybrid welding process was performed and the influence of liquid metal motion in the fusion zone on the results of calculations was analyzed.

Keywords: Solidification, Hybrid Welding, Fluid Flow, Numerical Modelling

1. Introduction

Hybrid welding process combines two welding methods: laser beam welding with classic electric arc welding. This modern technology due to a number of advantages compared to a single laser beam welding, has become very popular and is increasingly being used in the industry [1]. Hybrid welding process is mainly studied experimentally, while understanding and analysis of physical phenomena accompanying this process are still not fully understood and currently intensively studied [2, 3] since the understanding of physical phenomena occurring during hybrid welding process is essential for the proper use of this technology in practice.

Over the last several years in a number of works concerning the modeling of temperature field in welding and related processes, thermal, mechanical, electrical and metallurgical phenomena are often taken into consideration [3, 4]. However, recently the analysis is supplemented by fluid mechanics equations because of significant progress in computer sciences and development of new numerical techniques [2, 3].

The consideration of liquid material motion in the computational model allows for an analysis of previously neglected phenomena in welding processes associated with the dynamics of welding pool formation [3] and affects calculated temperature distribution in welded element, in consequence having significant influence on numerically estimated shape and size of the weld [2].

This work presents numerical model for convective motion of liquid material in the fusion zone and temperature field in welded plate by hybrid laser-arc welding method used in geometrical set-up with leading electric arc in the tandem. Differential governing equations describing analyzed thermal phenomena were numerically solved by Chorin's projection method with finite volume method (FVM) [5]. Analyzed domain was discretized by staggered grid, assuming laminar flow of viscous, incompressible

fluid. Temperature field and velocity field in the fusion zone were calculated. The influence of liquid material motion on the shape and size of the weld was analyzed in this study.

2. Mathematical model of liquid material motion in the fusion zone

The motion of liquid material resulting from the natural convection of a fluid (Boussinesq's model) is analyzed in the fusion zone limited by solidus temperature. In the area between the solidus and liquidus temperatures (T_S and T_L) liquid material motion is treated as a flow through porous medium in accordance with Darcy's model. The scheme of considered system is illustrated in figure 1.

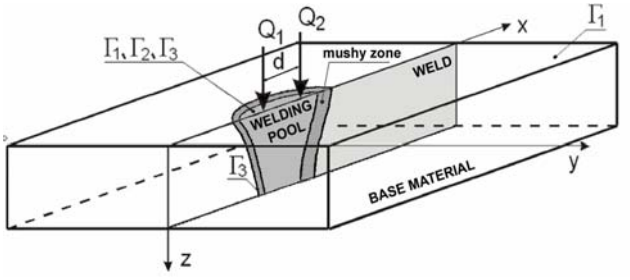

Fig. 1. Scheme of considered system

Velocity and temperature fields are obtained on the basis of solution into mass, momentum and energy conservation equations, defined as follows

$$\frac{\partial \rho}{\partial t}+\frac{\partial}{\partial x_\alpha}(\rho \mathbf{v})=0 \tag{1}$$

$$\frac{\partial(\rho u)}{\partial t}+\frac{\partial}{\partial x_\alpha}(\rho u \mathbf{v})=-\frac{\partial p}{\partial x}+\frac{\partial}{\partial x_\alpha}\left(\mu\frac{\partial u}{\partial x_\alpha}\right)-\frac{\mu u}{\rho K}$$

$$\frac{\partial(\rho v)}{\partial t}+\frac{\partial}{\partial x_\alpha}(\rho v \mathbf{v})=-\frac{\partial p}{\partial y}+\frac{\partial}{\partial x_\alpha}\left(\mu\frac{\partial v}{\partial x_\alpha}\right)-\frac{\mu v}{\rho K} \tag{2}$$

$$\frac{\partial(\rho w)}{\partial t}+\frac{\partial}{\partial x_\alpha}(\rho w \mathbf{v})=-\frac{\partial p}{\partial z}+\frac{\partial}{\partial x_\alpha}\left(\mu\frac{\partial w}{\partial x_\alpha}\right)+g\beta_T(T-T_S)-\frac{\mu w}{\rho K}$$

$$C\frac{\partial T}{\partial t}=\frac{\partial}{\partial x_\alpha}\left(\lambda\frac{\partial T}{\partial x_\alpha}\right)-C\frac{\partial T}{\partial x_\alpha}\mathbf{v}+\tilde{Q} \tag{3}$$

where ρ is a density [kg/m^3], g is gravity acceleration, β_T is thermal expansion coefficient [1/K], μ dynamic viscosity [kg/ms], K is porous medium permeability, $\lambda=\lambda(T)$ is thermal conductivity [W/mK], $C=C(T)$ is effective heat capacity with included latent heats associated with material's state change (solid-liquid and liquid-gas transformation), $\tilde{Q}=Q_1+Q_2$ is a volumetric heat source (Q_1 - eletric arc heat source and Q_2 - laser beam heat source), $\mathbf{v}=\mathbf{v}(x_\alpha,t)=(u,v,w)$ is a velocity vector, $T=T(x_\alpha,t)$ is a temperature and x_α is a material point coordinate.

Initial and boundary conditions complete the governing equations. Momentum conservation equation (2) is supplemented by $t=0:\mathbf{v}=0$ initial condition and Dirichlet boundary condition Γ_3: $\mathbf{v}=0$ implemented at the welding pool boundary, determined by solidus temperature. Energy conservation equation is completed by initial condition $t=0:T=T_0$ and boundary conditions of Neumman (for heat sources) and Newton boundary conditions with heat loss due to convection, radiation and evaporation taken into account

$$-\lambda\frac{\partial T}{\partial n}=\alpha(T-T_0)+\varepsilon\sigma(T^4-T_0^4)\Big|_{\Gamma_1}-q_o+q_v\Big|_{\Gamma_2} \tag{4}$$

where α is convective coefficient [W/m^{2}K], ε is radiation coefficient and σ is Stefan-Boltzmann constant. Element q_s is the heat flux towards the top surface of the welded element ($z=0$) in the source activity field, while q_v represents heat loss due to material evaporation in area where $T\geq T_L$, Γ is a boundary of analysed domain.

Temperature distribution, and also the motion of liquid material in the welding pool are mostly determined by the heat input delivered to the workpiece. In modelling of electric arc welding process proposed by Goldak [6] "double ellipsoidal" model is often used to describe heat source power distribution. This model defines heat source power distribution along two half-ellipsoids connected each other with one semi-axis. Goldak's heat source model is described by the following equation

$$Q_{1,2}=\begin{cases} q_1(x,y,z)=\dfrac{6\sqrt{3}f_1Q}{abc_1\pi\sqrt{\pi}}\times\exp(-3\dfrac{x^2}{c_1^2})\times & \text{for } x<x_o \\ \quad\times\exp(-3\dfrac{y^2}{a^2})\times\exp(-3\dfrac{z^2}{b^2}) & \\ q_2(x,y,z)=\dfrac{6\sqrt{3}f_2Q}{abc_2\pi\sqrt{\pi}}\times\exp(-3\dfrac{x^2}{c_2^2})\times & \text{for } x\geq x_o \\ \quad\times\exp(-3\dfrac{y^2}{a^2})\times\exp(-3\dfrac{z^2}{b^2}) & \end{cases} \tag{5}$$

where a, b, c_1 and c_2 [m] are set of axes defining front ellipsoid and rear ellipsoid, Q is the heat input [W], f_1 and f_2 ($f_1+f_2=2$) represents energy distribution at the front and the rear section of the heat source, thus resultant distribution of the source energy is the total sum described as $Q_1(x,y,z)=q_1(x,y,z)+q_2(x,y,z)$.

Laser beam power distribution is usually defined with Gaussian distribution along radial direction of the beam with heat source intensity decreasing with increasing its penetration in the material which refers to the melting mechanism in laser beam welding. A proper selection of Goldak's heat source parameters allows for a modeling of laser beam power distribution [7], by assuming the same geometrical parameters of energy distribution in radial direction $c_1=c_2=a$ and the same energy distribution factors $f_1=f_2=1$, which gives in the result a Gaussian distribution in radial direction with exponential decrease of heat source intensity in material penetration deep.

Assuming, that during melting and solidification of welded workpiece the area between solidus and liquidus temperatures (T_S and T_L) is composed of regular matrix of spherical grains submerged in liquid material and the liquid fraction (porosity coefficient) is approximated linearly in the mushy zone

$$f_L = \frac{T - T_S}{T_L - T_S} \tag{6}$$

porous medium permeability K in Darcy's model can be expressed by Carman – Kozeny formula [3, 8] in accordance with the following equation

$$K = K_0 \frac{f_L^3}{(1 - f_L)^2}; \quad K_0 = \frac{d^2}{180} \tag{7}$$

where d is an average solid particle diameter in mushy zone [m], K_0 is the base permeability [m^2].

In equation (3) latent heat associated with changes in material's state in temperature range $T \in [T_S; T_L]$ (solid - liquid transformation) and at temperatures exceeding the boiling point of steel $T \geq T_b$ (liquid - gas transformation). At temperatures not exceeding the melting temperature constant density and specific heat are assumed, thus effective heat capacity equals $C(T) = \rho_S c_S$. Between solidus and liquidus temperatures latent heat of fusion is taken into consideration with assumption of linear increase of solid fraction, which leads to the following formula

$$C(T) = \rho_{SL} c_{SL} + \rho_S \frac{H_L}{T_L - T_S} \text{ for } T \in [T_S; T_L] \tag{8}$$

where H_L [J/kg] is a latent heat of fusion [2, 8].

The product of density and specific heat in the mushy zone is determined by the following equation

$$c_{LS}\rho_{LS} = c_S \rho_S (1 - f_L) + c_L \rho_L f_L \tag{9}$$

Above T_L temperature heat capacity is the product of density and specific heat for the liquid phase $C(T) = \rho_L c_L$, while in temperatures exceeding boiling point of steel up to a maximum temperature of heating latent heat of evaporation is taken into account according to the following formula

$$C(T) = \rho_L c_L + \rho_L H_b \frac{df_{LG}(T)}{dT} \text{ for } T \geq T_b \tag{10}$$

where H_b [J/kg] is a latent heat of evaporation [2, 3] and the increase of the liquid phase f_{LG} in the liquid - gas region is approximated linearly

$$f_{LG} = \frac{T_{\max} - T}{T_{\max} - T_b} \tag{11}$$

Differential governing equations (1), (2) and (3) are solved numerically using finite volume method (FVM) in Chorin's projection. The analyzed area was discretized by staggered grid, where velocity components and pressure are calculated on the separate differential grids shifted each other [5]. In the staggered grid velocity components are calculated at nodal points placed in the middle of each control volume face, while the pressure, density and temperature are calculated at the centre of control volume. Elementary control volume is shown in figure 2.

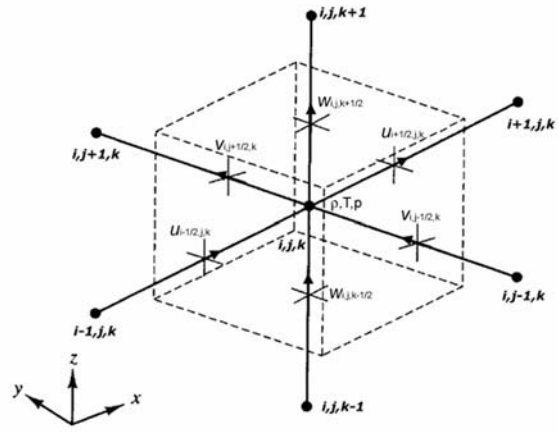

Fig. 2. Elementary control volume in a staggered grid

In the first step of the projection momentum equation is explicitly solved without momentum changes due to pressure forces. For elementary control volume (fig. 2) differential form of momentum equation is described as follows:

$$\begin{aligned}
u^*_{i+1/2,j,k} &= u^s_{i+1/2,j,k} + \\
&+ \Delta t^s \left(-(A_x)^s_{i+1/2,j,k} + (f_x)^s_{i+1/2,j,k} \frac{2}{\rho^s_{i+1,j,k} + \rho^s_{i,j,k}} \left((D_x)^s_{i+1/2,j,k} + (S_x)^s_{i+1/2,j,k} \right) \right) \\
v^*_{i,j+1/2,k} &= v^s_{i,j+1/2,k} + \\
&+ \Delta t^s \left(-(A_y)^s_{i,j+1/2,k} + (f_y)^s_{i,j+1/2,k} \frac{2}{\rho^s_{i,j+1,k} + \rho^s_{i,j,k}} \left((D_y)^s_{i,j+1/2,k} + (S_y)^s_{i,j+1/2,k} \right) \right) \\
w^*_{i,j,k+1/2} &= w^s_{i,j,k+1/2} + \\
&+ \Delta t^s \left(-(A_z)^s_{i,j,k+1/2} + (f_z)^s_{i,j,k+1/2} \frac{2}{\rho^s_{i,j,k+1} + \rho^s_{i,j,k}} \left((D_z)^s_{i,j,k+1/2} + (S_z)^s_{i,j,k+1/2} \right) \right)
\end{aligned} \tag{12}$$

where $\mathbf{v}^* = (u^*, v^*, w^*)$ is the velocity calculated from changes of velocity $\mathbf{v}^s$ resulting from advection $A_\alpha = (A_x, A_y, A_z)$, viscosity $D_\alpha = (D_x, D_y, D_z)$, source term $f_\alpha = (f_x, f_y, f_z)$ and flow through porosity medium $S_\alpha = (S_x, S_y, s_z)$.

Central difference quotients derived for staggered grid were used to calculate each term in equation (12). In the second step the projection $\mathbf{v}^*$ onto velocity vector $\mathbf{v}^{s+1} = (u^{s+1}, v^{s+1}, w^{s+1})$ is made using the following equation

$$u_{i+1/2,j,k}^{s+1} = u_{i+1/2,j,k}^{*} - \left(\frac{2\Delta t^s}{\rho_{i+1,j,k}^s + \rho_{i,j,k}^s}\right)\frac{p_{i+1,j,k} - p_{i,j,k}}{h_x}$$
$$v_{i,j+1/2,k}^{s+1} = v_{i,j+1/2,k}^{*} - \left(\frac{2\Delta t^s}{\rho_{i,j+1,k}^s + \rho_{i,j,k}^s}\right)\frac{p_{i,j+1,k} - p_{i,j,k}}{h_y} \quad (13)$$
$$w_{i,j,k+1/2}^{s+1} = w_{i,j,k+1/2}^{*} - \left(\frac{2\Delta t^s}{\rho_{i,j,k+1}^s + \rho_{i,j,k}^s}\right)\frac{p_{i,j,k+1} - p_{i,j,k}}{h_z}$$

with the assumption of fulfilling the continuity equation in the differential form

$$\frac{u_{i+1/2,j,k}^{s+1} - u_{i-1/2,j,k}^{s+1}}{h_x} + \frac{v_{i,j+1/2,k}^{s+1} - v_{i,j-1/2,k}^{s+1}}{h_y} + \frac{w_{i,j,k+1/2}^{s+1} - w_{i,j,k-1/2}^{s+1}}{h_z} = 0 \quad (14)$$

where h_x, h_y, h_z are the dimensions of control volume, Δt^s is a time step from the time s.

Equations (13) and (14) are deposited in a single Poison equation, from which pressure is calculated.

After velocity field of melted material is obtained, temperature field in welded workpiece is calculated on the basis of the solution of energy conservation equation, which in the differential form is expressed as follows

$$T_{i,j,k}^{s+1} = T_{i,j,k}^{s} + \frac{\tilde{Q}\Delta t^s}{C} - \left(u\frac{T_{i+1}^s - T_{i-1}^s}{2h_x} + v\frac{T_{j+1}^s - T_{j-1}^s}{2h_y} + w\frac{T_{k+1}^s - T_{k-1}^s}{2h_z}\right)\Delta t^s +$$
$$+ \frac{\Delta t^s}{C}\left(\frac{\lambda_{i+1}^s - \lambda_{i-1}^s}{2h_x}\frac{T_{i+1}^s - T_{i-1}^s}{2h_x} + \lambda_i^s\frac{T_{i-1}^s - 2T_i^s + T_{i+1}^s}{(h_x)^2}\right) + \quad (15)$$
$$+ \frac{\Delta t^s}{C}\left(\frac{\lambda_{j+1}^s - \lambda_{j-1}^s}{2h_y}\frac{T_{j+1}^s - T_{j-1}^s}{2h_y} + \lambda_j^s\frac{T_{j-1}^s - 2T_j^s + T_{j+1}^s}{(h_y)^2}\right) +$$
$$+ \frac{\Delta t^s}{C}\left(\frac{\lambda_{k+1}^s - \lambda_{k-1}^s}{2h_z}\frac{T_{k+1}^s - T_{k-1}^s}{2h_z} + \lambda_k^s\frac{T_{k-1}^s - 2T_k^s + T_{k+1}^s}{(h_z)^2}\right)$$

Because forward Euler integration scheme is used in calculations as well as central difference quotients, quality of the results depends on the conditions of stability. To ensure proper quality of the results solution algorithms are taking into account the time step constraints and if necessary introduce additional stabilization algorithms for high Peclet numbers [5].

3. Results of calculations

On the basis of developed solution algorithms numerical analysis of melted material velocity field and temperature field in welded workpiece was performed for laser-arc hybrid welded plate. Thermo-physical parameters assumed in the calculations are presented in table 1.

Simulations have been performed for butt-welded plate with dimensions 150x30x4mm by laser-arc in the geometrical set-up with leading electric arc in the tandem. In the calculations Goldak's double ellipsoidal heat source model was used to describe electric arc as well as laser beam power distribution. The following technological parameters were assumed in analysis: electric arc power Q_A = 6.6 kW, c_1 = 4 mm, c_2 = 8 mm, a = 3 mm, b = 2 mm, f_1 = 0.4, f_2 = 1.6 and laser beam power Q_L = 3.8 kW, $c_1 = c_2 = a$ = 1 mm, b = 7 mm, $f_1 = f_2$ = 1. The distance between the laser beam and electric arc was set to d = 4 mm and welding speed v = 2.6 m/min.

Table 1.
Thermo-physical parameters assumed in computer simulations

Nomenclature	Symbol	Value
Solidus temperature	T_S	1750
Liquidus temperature	T_L	1800
Boiling point	T_b	3010
Ambient temperature	T_0	293
Specific heat of solid phase	c_S	650
Specific heat of liquid phase	c_L	840
Density of solid phase	ρ_S	7800
Density of liquid phase	ρ_L	6800
Latent heat of fusion	H_L	$270\text{x}10^3$
Latent heat of evaporation	H_b	$76\text{x}10^5$
Thermal conductivity of solid phase	λ_S	40
Thermal conductivity of liquid phase	λ_L	25
Convective heat transfer coefficient	α	50
Boltzmann's constant	σ	$5.67\text{x}10^{-8}$
Thermal expansion coefficient	β_T	$4.95\text{x}10^{-5}$
Surface radiation emissivity	ε	0.5
Dynamic viscosity	μ	0.006
Average solid particle diameter	d_0	0.0001

Temperature field in welded plate and velocity field of liquid steel in the welding pool are presented in figure 3, in the longitudinal section of the joint at the middle of heat sources activity zone. This figure shows the formation of the fusion zone at different simulation time. Solid black line (fig 3a) determines fusion zone boundary (T_S) within motion of liquid steel is analyzed. Two areas of fluid circulation are observed in the melted zone (fig. 3b). First area is formed due to melting of the material by the arc and the second due to action of the laser beam. Maximum velocities of molten metal are found in the laser beam activity zone (fig 3b). Based on temperature distribution it can also be observed that the arc heat source in this system melts the upper layers of the material up to 1.5mm deep into the plate, while the full penetration of the material is obtained by the action of a laser beam.

Temperature field and velocity field in the fusion zone are also illustrated in figure 4 at the cross section of the joint. At the left side of the figure temperature field is illustrated with pointed out fusion zone boundary (black solid line), in the other hand the right side of this figure shows velocity field of liquid steel within the fusion zone. The results are presented in the area of material melting by the arc (fig. 4a) and by the laser beam (fig. 4b). Higher velocity of molten metal is found in the laser beam activity zone (fig 4b), moreover in this zone full material penetration is obtained.

The influence of fluid flow in the welding pool on simulation results was analyzed. Computer simulation of hybrid welding was performed with and without consideration of the liquid material motions in the fusion zone. Results of calculations are illustrated in figure 5 and figure 6.

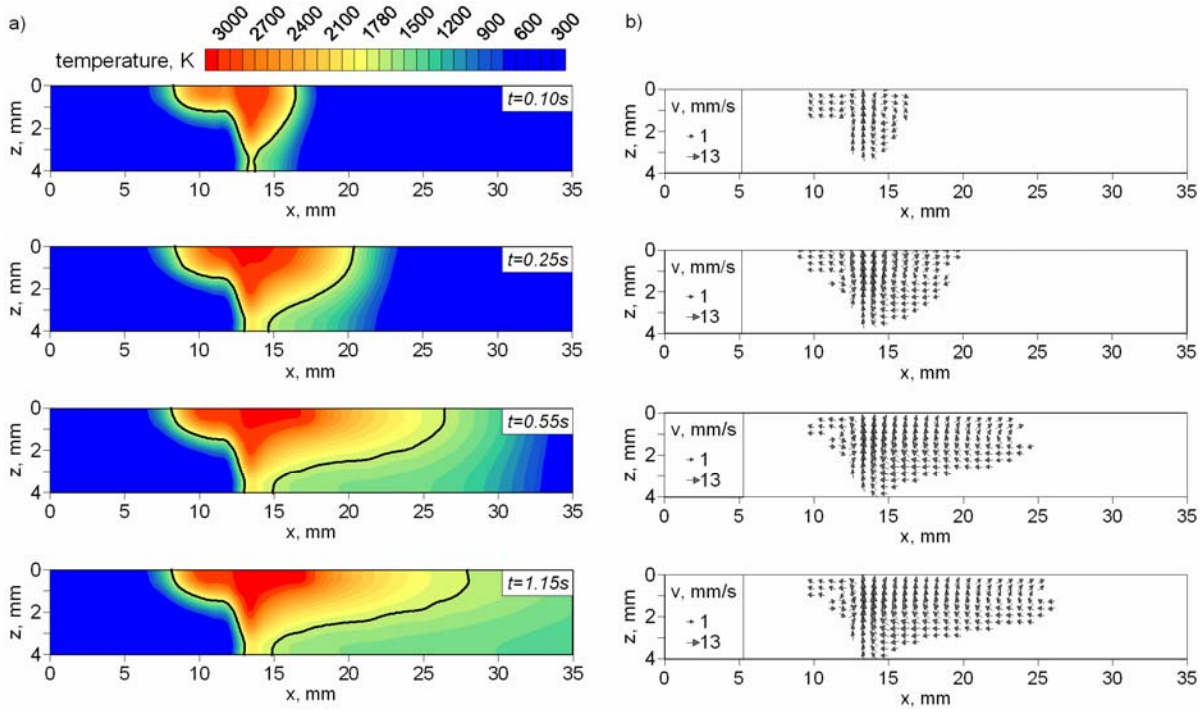

Fig. 3. Distribution of a) temperature and b) velocity of liquid steel in the longitudinal section of welded plate (in the middle of heat sources activity zone, y=0) at different times of simulation

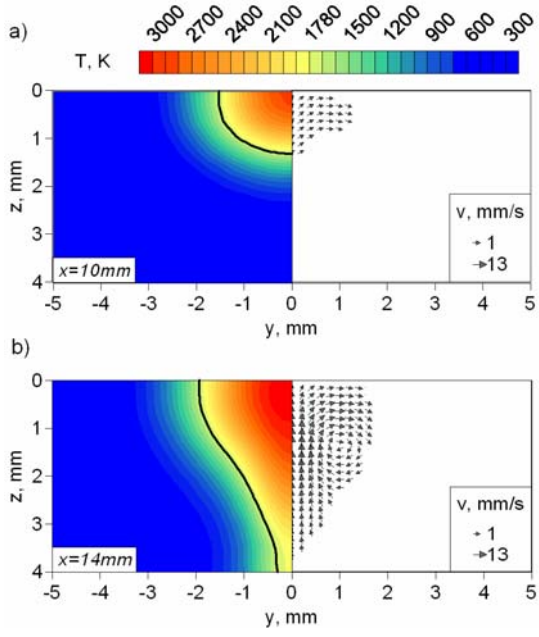

Fig. 4. Temperature field and melted material velocity field in the cross section of the weld melted by a) electric arc and b) laser beam

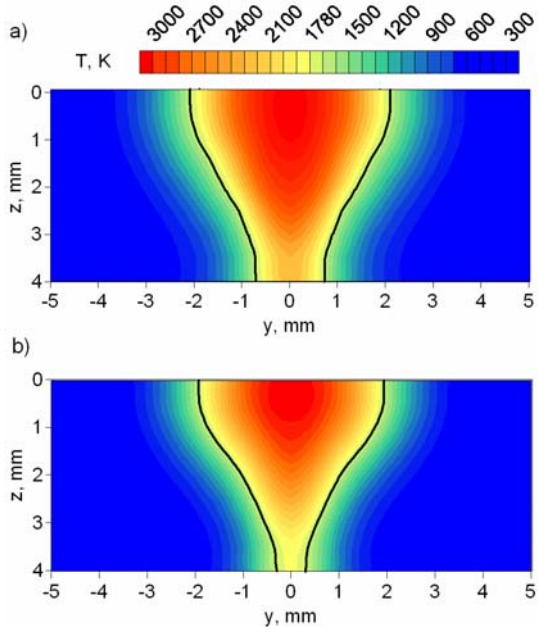

Fig. 5. Temperature field in cross section of welded joint. Simulation made a) without and b) with motion of melted material taken into considerations

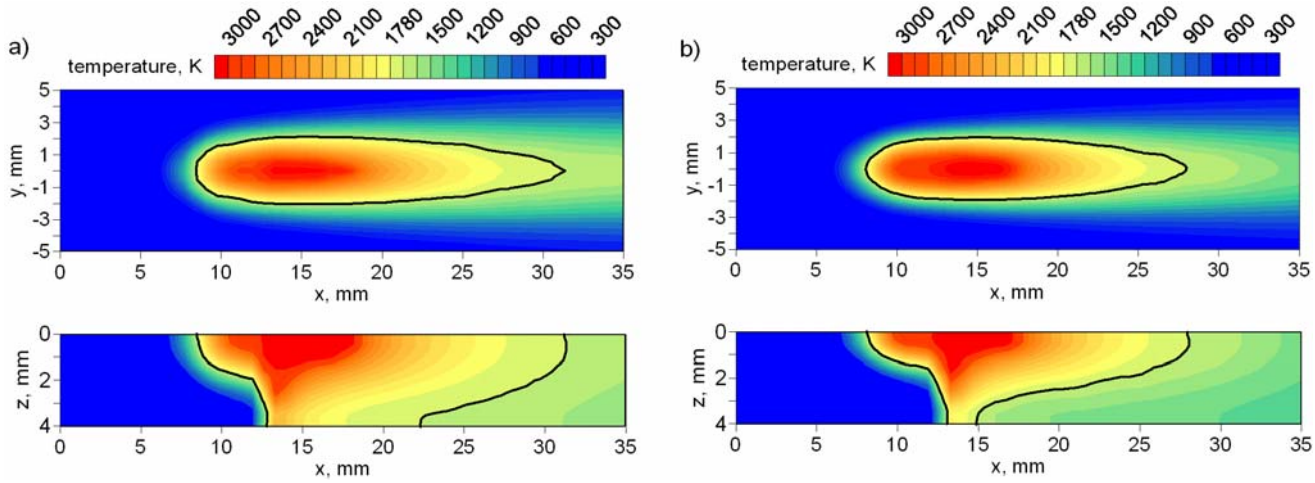

Fig. 6. Temperature field at the top surface (from the face of the weld) and in longitudinal section of welded joint. Simulation made a) without and b) with motion of melted material taken into considerations

Presented results show significant influence of liquid metal motion on the results of calculations. Numerically estimated size of the joint is wider in simulations made without consideration of liquid material flow in the fusion zone (fig. 5) and the welding pool is larger (fig. 6).

4. Conclusions

Consideration of liquid material motion in fusion zone is important in the simulation of welding processes. Due to the fact that temperature distribution determines the shape and size of the weld, equations of fluid mechanics taken into account in the analysis provides changes in estimated geometry of the weld.

The developed numerical model is a basis for studying the dynamics of the weld pool during laser-arc hybrid welding.

References

[1] J. Pilarczyk, M. Banasik, J. Dworak, S. Stano, Hybrid welding using laser beam and electric arc, Przegląd Spawalnictwa, 10, (2007) 44-48 (in Polish)

[2] W. Piekarska, M. Kubiak, The numerical analysis of thermal phenomena in hybrid laser-arc welding process with convective motion in the melted zone, Metalurgija, 49, 2 (2010) 456-460

[3] J. Zhou, H.L. Tsai, Modeling of transport phenomena in hybrid laser – MIG keyhole welding, International Journal of Heat and Mass Transfer, 51 (2008) 4353-4366.

[4] A. Bokota, W. Piekarska, Stress in the heat affected zone of laser welded joint with preheating, Technologia i Automatyzacja Montażu, 3/4 (2004) 86-90 (in Polish)

[5] S.V. Patankar, Numerical heat transfer and fluid flow, Taylor & Francis, USA (1990)

[6] J.A. Goldak, Computational Welding Mechanics, Springer NY (2005)

[7] A. De, S.K. Maiti, C.A. Walsh, K.D.H. Bhadesia, Finite element simulation of laser spot welding, Science Technology of Welding and Joining, 8, 5 (2003) 377-384

[8] R. Parkitny, T. Skrzypczak, Simulation of solidification of two component alloys with solute distribution, Archives of Foundry, 2, 4 (2002) 198-203

Modelowanie numeryczne ruchu ciekłego materiału w strefie przetopienia złącza spawanego hybrydowo

Streszczenie

Praca dotyczy modelowania ruchu ciekłego metalu w strefie przetopienia złącza spawanego doczołowo techniką hybrydową laser-łuk elektryczny. Pole prędkości w strefie przetopienia i pole temperatury w spawanym płaskowniku otrzymano z rozwiązania równań zachowania masy, pędu i energii. Do rozwiązania równań różniczkowych wykorzystano projekcję Chorina i metodę objętości skończonych. W obliczeniach uwzględniono procesy topienia i krzepnięcia złącza z założeniem rozmytego frontu krzepnięcia gdzie ruch cieczy traktowano jako przepływ przez medium porowate. Do opisu rozkładu mocy łuku elektrycznego i wiązki laserowej wykorzystano „podwójnie elipsoidalny" model źródła ciepła. Na podstawie opracowanych algorytmów przeprowadzono symulację procesu spawania hybrydowego analizując wpływ ruchu ciekłego metalu w strefie przetopienia na wyniki obliczeń.